Priming therapy by targeting enhancer-initiated pathways in patient-derived pancreatic cancer cells

Nicolas A. Fraunhoffer,[a,b,c,m] Aura I. Moreno Vega,[d,m] Analía Meilerman Abuelafia,[a] Marie Morvan,[e] Emilie Lebarbier,[e,f] Tristan Mary-Huard,[f] Michael T. Zimmermann,[g,h] Gwen Lomberk,[g,h] Raul Urrutia,[g,h] Nelson Dusetti,[a] Yuna Blum,[i,n] Remy Nicolle,[d,j,n] and Juan Iovanna[a,k,l,n,*]

[a]Centre de Recherche en Cancérologie de Marseille (CRCM), INSERM U1068, CNRS UMR 7258, Parc Scientifique et Technologique de Luminy, Aix-Marseille Université and Institut Paoli-Calmettes, Marseille, France
[b]Universidad de Buenos Aires, Consejo Nacional de Investigaciones Científicas y Técnicas, Centro de Estudios Farmacológicos y Botánicos (CEFYBO), Facultad de Medicina, Buenos Aires, Argentina
[c]Universidad de Buenos Aires, Facultad de Medicina, Departamento de Microbiología, Parasitología e Inmunología, Buenos Aires, Argentina
[d]Tumour Identity Card Program (CIT), French League Against Cancer, Paris, France
[e]Laboratoire Modal'X - UMR 9023, Université Paris Nanterre, Nanterre, France
[f]Université Paris-Saclay, AgroParisTech, INRAE, UMR MIA Paris-Saclay, Palaiseau 91120, France
[g]Genomics and Precision Medicine Center (GSPMC), Medical College of Wisconsin, Milwaukee, WI, USA
[h]Division of Research, Department of Surgery, Medical College of Wisconsin, Center, Milwaukee, WI, USA
[i]Univ Rennes, CNRS, INSERM, IGDR (Institut de Génétique et Développement de Rennes) - UMR 6290, ERL U1305, Rennes, France
[j]Université Paris Cité, Centre de Recherche sur l'Inflammation (CRI), INSERM, U1149, CNRS, ERL 8252, Paris F-75018, France
[k]Hospital de Alta Complejidad El Cruce, Florencio Varela, BA, Argentina
[l]University Arturo Jauretche, Florencio Varela, BA, Argentina

Summary

Background Systems biology leveraging multi-OMICs technologies, is rapidly advancing development of precision therapies and matching patients to targeted therapies, leading to improved responses. A new pillar of precision oncology lies in the power of chemogenomics to discover drugs that sensitizes malignant cells to other therapies. Here, we test a chemogenomic approach using epigenomic inhibitors (epidrugs) to reset patterns of gene expression driving the malignant behavior of pancreatic tumors.

Methods We tested a targeted library of ten epidrugs targeting regulators of enhancers and super-enhancers on reprogramming gene expression networks in seventeen patient-derived primary pancreatic cancer cell cultures (PDPCCs), of both basal and classical subtypes. We subsequently evaluated the ability of these epidrugs to sensitize pancreatic cancer cells to five chemotherapeutic drugs that are clinically used for this malignancy.

Findings To comprehend the impact of epidrug priming at the molecular level, we evaluated the effect of each epidrugs at the transcriptomic level of PDPCCs. The activating epidrugs showed a higher number of upregulated genes than the repressive epidrugs (χ^2 test p-value <0.01). Furthermore, we developed a classifier using the baseline transcriptome of epidrug-primed-chemosensitized PDPCCs to predict the best epidrug-priming regime to a given chemotherapy. Six signatures with a significant association with the chemosensitization centroid (R ≤ −0.80; p-value < 0.01) were identified and validated in a subset of PDPCCs.

Interpretation We conclude that targeting enhancer-initiated pathways in patient-derived primary cells, represents a promising approach for developing new therapies for human pancreatic cancer.

*Corresponding author. Centre de Recherche en Cancérologie de Marseille (CRCM), INSERM U1068, CNRS UMR 7258, Parc Scientifique et Technologique de Luminy, Aix-Marseille Université and Institut Paoli-Calmettes, Marseille, France.
E-mail address: juan.iovanna@inserm.fr (J. Iovanna).
[m]These authors contributed equally to this work.
[n]Co-last authors.

Research in context

Evidence before this study
PDAC is the most lethal type of pancreatic cancer. This type of cancer is refractory for the current treatments. The tumor phenotype is a strong determinant of the drug response. Furthermore, epigenomic landscapes are the main regulators of phenotype-driver pathways.

Added value of this study
This study extensively analyses the effect of epigenetic modulation on the transcriptomic phenotype and

chemoresistant profile of PDAC. Moreover, we proposed novel strategies to improve the chemotherapeutic response by applying priming epigenetic modulation.

Implications of all the available evidence
These results provide new insights to improve the chemotherapeutic response of PDAC patients, elaborating novel combinatory therapies against chemoresistance phenotype.

Introduction

Pancreatic Ductal Adenocarcinoma (PDAC) is one of the most aggressive malignant diseases with a current worldwide mortality-incidence ratio of 94.2%. More importantly, PDAC is projected to become the second most frequent cause of cancer deaths before 2030,[1,2] significantly increasing its public health impact. Chemotherapy remains the standard treatment for most advanced and metastatic PDAC. While precision oncology brought a renewed enthusiasm for advances in targeted and immune-therapies,[3,4] the outlook for PDAC patients has remained similar across the last 40 years.

The emerging field of precision oncology based its initial predictions for the potential benefit of distinct therapies on gene mutations. However, genetic mutations while important for PDAC development and progression, have failed to robustly predict therapy responses.[4–6] This ascertainment has renewed the interest in chemogenomics, namely the study of the genome-wide response of a biological system to chemical compounds, often discovered through screening either targeted or non-targeted chemical libraries. Thus, chemogenomics often refers to both the concept of changing the genome-wide transcriptional landscape and the methodology used to screen compounds that display this effect. Simultaneously to these developments, epigenomic mechanisms driving enhancer-promoter coupling emerged as factors of paramount importance in PDAC initiation, promotion, progression, and chemoresistance.[4,7–10] Thus, this knowledge became the rational of the current study that seeks to modify the genome-wide transcriptional landscape of pancreatic cancer cells by targeting epigenomic regulators, of enhancer pathways, which by their own nature, are well-known as cell reprogramming factors.

The dynamic regulation for the assembly and disassembly of both types of enhancers, namely those mediated by either H3K9 or H3K27, is critical for the activation and silencing of promoters. Biochemically, the activation and inactivation of these two types of

promoters are achieved through acetylation or methylation of both lysine residues, through Histone Acetyl and Methyl Transferases, respectively. Reversal of these events are mediated by histone deacetylases and demethylases. These enhancers regulate gene promoters that drive the distinct gene expression landscapes, which can give rise to either basal or classical pancreatic cancer. This functional link between enhancers with promoters and gene bodies is achieved through H3K4- and H3K36-regulating enzymes.

The rapid emergence of available new drugs that target these epigenomic regulatory mechanisms warrants their testing in pancreatic cancer.[8] Consequently, the current study tests an approach involving the priming of patient-derived pancreatic cancer cells with epidrugs that target H3K9 and H3K27 enhancers alone or in groups (super-enhancers) to reprogram gene expression landscapes, with the aim of sensitization to standard chemotherapy. The assembly and disassembly of these enhancers appear to function as a type of checkpoint for also coupling to promoters and gene bodies. Thus, the pharmacological targeting of these mechanisms may reprogram the transcriptomic landscape of cancer cells to better respond to treatments. We evaluate the effect of ten different epidrugs based on their ability to impact both types of enhancers, using primary cultured naïve pancreatic tumor cells of either the basal or classical phenotype, obtained from 17 different affected patients. The results from these experiments strongly support the validity of this approach for achieving beneficial effects on pancreatic cancer cells from patients. As importantly this approach allowed us to design and propose a new classifier that can help predict the best epidrug-priming regime that would sensitize naïve, untreated primary cells, to a given chemotherapy. Therefore, the concepts, approach, methodology, and analyses described in this article offer a new framework for further investigation, a valued goal of precision oncology when facing the increased incidence of this disease predicted for the following decades.

Methods

Patient-derived primary pancreatic cancer cell cultures (PDPCCs)

PDPCCs were obtained from patient-derived xenograft (PDX). PDAC samples were obtained from three expert clinical centers under the PaCaOmics clinical trial (number 2011-A01439-32) after receiving ethics review board approval. Consent forms of informed patients were collected and registered in a central database. Animal experimental procedures were conducted according to the Directive 2010/63/EU in the Stabulation and Animal Experimentation Platform (PSEA, Scientific Park of Luminy, Marseille) and were approved by the ethics committee (EC N°14, Marseille) (Project #9562-2016051914513578). PDXs were generated through the subcutaneous implantation of PDAC samples with matrigel in NMRI-nude mice until the tumor reached a 1 cm^3 (Swiss Nude Mouse Crl: NU(lco)-Foxn1nu; Charles River Laboratories, Wilmington, MA). PDPCCs were obtained from splitted PDXs into small pieces of 1 mm^3 and dissociated with collagen type V (C9263; Sigma-Aldrich, Inc., St. Louis, Missouri, USA) and trypsin/EDTA (25200-056; Gibco, Thermo Fisher, Waltham, Massachusetts, USA). Cell homogenate was resuspended in DMEM with 1% w/w penicillin/streptomycin (Gibco, Life Technologies) and 10% of fetal bovine serum (Lonza). After centrifugation, cells were re-suspended in Serum Free Ductal Media (SFDM)[5] and conserved at 37 °C in a 5% CO_2 incubator.

Isolation and primary culture of cancer-associated fibroblasts (CAFs)

The CAFs used in this study were isolated by Leca et al.[11] Briefly, the tumors were cut into small pieces of 1 mm^3 and the pieces were dissociated using the Tumor Dissociation Kit (130-095-929; Miltenyi Biotec). Then, cells were passed through a cell strainer (100 μM), and finally plated into a T75 flask. Cells were cultured in DMEM/F12 medium (31330-038; Gibco, Thermo Fisher, Waltham, Massachusetts, USA), 10% serum, 2 mmol/l L-glutamine (25030-024; Gibco, Thermo Fisher, Waltham, Massachusetts, USA), 1% antibiotic-antimycotic (15240-062; Gibco, Thermo Fisher, Waltham, Massachusetts, USA), and 0.5% sodium pyruvate (11360-039; Gibco, Thermo Fisher, Waltham, Massachusetts, USA).

PDPCC priming with epidrugs and chemotherapy treatment

Ten to seventeen PDPCCs were treated in a biphasic regimen with ten epidrugs and five chemotherapeutic drugs. Initially, two thousand cells per well were seeded in 96-well plates in SFDM. Twenty-four hours later, the media was supplemented with the epidrug for 72 h. The control wells were supplemented with DMSO (vehicle). After that, the media with epidrug was replaced with the media contained increasing concentrations of the chemotherapeutic drug and incubated for 72 h. Control

PDPCCs received normal cell media at this stage. All the drugs were administrated with Tecan D300e drug dispenser (Tecan, Mannedorf, Switzerland) and the wells were distributed randomly. Cell viability was measured with PrestoBlue (Thermo Fisher, Waltham, Massachusetts, USA) reagent and quantified using the plate reader Tristar LB941 (Berthold Technologies, Bad Wildbad, Germany). For each PDPCC-epidrug-chemotherapy, the dose response curves were calculated using the GRmetrics R package (version 1.14.0) and normalized to control samples. The concentration at which epidrugs were used and their target enzymes (in brackets) were as follows: C646 (3.4 μmol/L; P300; Selleckchem, Houston, TX, USA), Chaetocin (10 nmol/L; SUV39H1/2; Selleckchem, Houston, TX, USA), CPI1205 (50 μmol/L; EZH2), CPI455 (24 μmol/L; KDM5A/B/C; Selleckchem, Houston, TX, USA), GSK2879552 (50 μmol/L; KDM1A; Adooq Bioscience, Irvine, CA, USA), GSKJ1 (50 μmol/L, KDM6A/B; Adooq Bioscience, Irvine, CA, USA), ML324 (9.7 μmol/L; KDM4; Selleckchem, Houston, TX, USA), OICR9429 (50 μmol/L; WDR5; Selleckchem, Houston, TX, USA), RGFP966 (12 μmol/L; HDAC3; Selleckchem, Houston, TX, USA), and WDR50103 (50 μmol/L; WDR5; Adooq Bioscience, Irvine, CA, USA). Four concentrations were used for the chemotherapeutic drugs. For gemcitabine, 5-fluorouracil, oxaliplatin, and irinotecan the range was from 0.1 μmol/L to 1000 μmol/L, whereas for docetaxel was from 0.01 μmol/L to 100 μmol/L and for the active metabolite of irinotecan (SN-38), was from 0.0001 μmol/L to 0.01 μmol/L.

RNA extraction and RNA-seq analysis

To evaluate the impact of the epidrugs on the transcriptomic profiles, the PDPCC were treated with the epidrugs previous to RNA extraction. Briefly, two hundred thousand cells were seeded on a T25 flask in SFDM. Twenty-four hours later the media was supplemented with the epidrug and incubated for 72 h. Control samples were treated with DMSO only. PDPCCs RNA was extracted with RNeasy Mini Kit (Qiagen). RNA libraries were prepared (Illumina NovaSeq 6000 S1 Reagent Kit v1.5) and run on the Illumina NovaSeq 6000 for 100 bp paired end reads. RNAseq reads were mapped using STAR and SMAP on the human hg19 and mouse mmu38. Gene expression profiles were obtained using FeatureCount. Gene counts were normalized using the upper-quartile approach. The sample inclusion criteria were: 1- at least 10 million human reads, 2- less than 10% of murine reads, and 3- paired epidrug-control samples.

Differential gene expression analysis

Gene expression levels between epidrug-primed and control PDPCCs were compared using the DESEq2 Bioconductor package (version 1.28.1). A differential analysis was performed to identify up/down-regulated genes, followed by a Benjamini–Hochberg multiple

testing procedure to control the FP error rate at a nominal level of 5%. Upregulated genes were defined as those having a positive $\log_2$FC (>0) whereas downregulated genes as those having a negative $\log_2$FC (<0). A gene list ranked on the DESeq2 Wald-statistic derived from the comparison of expression levels between epidrug-primed vs. ctrl PDPCCs was also derived.

Functional analysis

With the aim of identifying the set of biological pathways significantly altered following epidrug priming of PDPCCs, a gene set enrichment analysis (fGSEA Bioconductor package, version 1.14.0) was carried out on the genes list previously ranked on the DESeq2 Wald-statistic (derived from the comparison of expression levels between epidrug-primed vs. control PDPCCs). Normalized enrichment score (NES) obtained following GSEA analysis represented the extent to which a biological pathway was found to be overrepresented at the top or bottom of the list of pre-ranked genes. In this way, positive NES values would represent a pathway significantly enriched in genes whose expression is higher in epidrug-primed PDPCCs, and vice versa for negative NES values. Pathways were considered significantly enriched with an adjusted p-value ≤ 0.05. Signaling pathways used were obtained from the KEGG 2019 Human and Reactome 2016.

Histone mark and chromatin state enrichment analysis

We wished to evaluate which histone marks and chromatin states (defined by specific combinations of histone marks) would be significantly overrepresented at a proximal or distal distance of the transcription start site (TSS) of genes impacted upon epidrug priming of PDPCCs. We thus carried out an GSEA analysis on genes pre-ranked on the Wald-statistic from the differential expression analysis of epidrug-primed vs. control PDPCCs. Proximal distances to the TSS of a given gene were defined as 2 kb upstream of TSS and 500 b downstream of TSS whilst distal distances were defined as 10 kb upstream of TSS and 1 kb downstream of TSS. In this context, a positive NES obtained following GSEA analysis would represent a significant enrichment of a given histone mark/chromatin state in genes found more highly expressed in epidrug-primed PDPCCs vs. control (and vice versa for a negative NES). Signatures of histone marks and chromatin states associated with the TSS of a given gene were obtained from our previous analysis of 26 PDAC patient-derived xenografts.[8]

Chemosensitivity score calculation: SBliss and ECGain

The SBliss synergy score was calculated as the excess of the observed effect of a drug combination over the expected effect of each drug acting independently, as stated by the Bliss model.[12] Under this reasoning, if we define the combined inhibitory effect of the combination of two drugs as y_c, and y_e as the expected effect if they were acting independently, the synergy score was calculated as:

$$S_{Bliss} = \gamma_c - \gamma_e = \left(1 - \frac{Cellcount\,Epi\,day6}{Cellcount\,DMSO\,day6}\right) \cdot 100$$

An S_{Bliss} score was calculated for each of the four concentrations of a specific chemotherapeutic drug, 'combined' with a single concentration of a given epidrug.

The ECGain was defined as the global impact that the epidrug priming had on the chemotherapy efficacy. More specifically, it was measured as the gain of detrimental impact on cell viability between epidrug priming followed by chemotherapeutic drug (referred to as Epi-Chemo) vs. chemotherapeutic drug alone (Chemo). Like the SBliss, the ECGain was calculated for each of the four concentrations of a given chemotherapeutic drug and the single concentration of an epidrug.

$$ECGain\,ECCGain = 1 \cdot (\gamma_c - \gamma_e)$$

Mean values of the SBliss and ECGain scores were then used to compare samples (mean of the scores calculated for each of the chemotherapeutic drug concentrations).

Chemosensitivity signature identification

Gene signatures of synergic chemosensitization were derived from the differential analysis of baseline transcriptomes (untreated cells) between PDPCCs experimentally sensitized to a given chemotherapy after epidrug priming vs. non-sensitized cells. Only Epi-Chemos where at least 2 PDPCCs were observed to be chemosensitized by epidrug-priming were eligible for differential analysis. In detail, a differential expression analysis was carried out using DESeq2 to identify genes presenting a statistically significant difference (FDR 5%) of baseline expression levels between chemosensitized vs. non-chemosensitized PDPCCs. EpiChemos where at least 50 DEGs were observed were selected and synergy signatures were established from the top 1000 most deregulated genes.

Nearest-centroid classifier

To classify treatment-naïve PDPCCs as chemosensitizable by epidrug-priming or not, we built a nearest-centroid predictor[5] from centroids calculated for chemosensitized PDPCCs and not chemosensitized PDPCCs. More specifically, the centroids for chemosensitized and not chemosensitized PDPCCs for a given EpiChemo were each calculated as the mean of expression levels for all the 1000 genes belonging to a specific EpiChemo sensitivity signature. Independent transcriptomic data (RNAseq) from untreated PDPCCs was

then used to assign a class to each primary cell culture defined by the Pearson correlation between the mean expression profile for a given PDPCC and the formerly established centroids. PDPCCs with a delta of Pearson correlation coefficient in the upper-quartile were predicted to be chemosensitizable by epidrug priming (predicted chemosensitized). Inversely, those with a delta of Pearson correlation coefficient in the lower-quartile were predicted not to present a chemosensitization following epidrug priming (predicted not-chemosensitized).

Software and statistical analyses

Data analysis was performed R (4.0.3) and RStudio (Version 1.1.453) with the packages described in the methods. Spearman and Pearson correlation coefficients and the significance levels were calculated using the Hmist R package. Linearity and normally assumptions were tested using scatterplot and Shapiro–Wilk test. Wilcoxon matched-pairs signed rank test was performed with R basic functions. All the p-values below 0.05 were considered significant. Raw codes will be made available from the corresponding author upon reasonable request.

Data availability

The authors declare that all relevant aggregate data supporting the findings of this study are available within the article and its supplementary information files.

Role of the funding source

The funders had no role in study design, data collection, data analyses, interpretation, or writing of this report. The views expressed in this manuscript are those of the authors and do not necessarily represent the views of the INCa, Canceropole PACA; the Amidex Foundation; or INSERM. The corresponding authors had full access to all the data and take final responsibility for the decision to submit for publication. None of the contributing authors was denied access to the data of this study.

Results

Enhancers targeting drugs primarily affect gene cell cycle regulatory gene expression networks

We evaluated the effects of compounds that target regulators of the H3K9 and H3K27-mediated enhancers. For this purpose, we used a unique set of 17 different patient-derived pancreatic cancer cells of the basal-like (64.7%, n = 11) and classical (35.3%, n = 6) subtypes (Fig. 1a). We incubated cells for 72 h to ensure at least once their transit through S phases where histone marks undergo semi-conservative duplication so that changes achieved during this priming period are at least partially inherited in daughter cells. We tested ten different epidrugs inhibiting each distinct enzymes involved in modifying both types of enhancers (Fig. 1b). Based on the drug being targeted and predicted effect, they were

further categorized into primarily activating vs. repressing. Accordingly, activating agents were expected to result in a larger global upregulation of gene expression and vice versa. RNAseq analysis of primed PDPCC vs. control revealed varied and distinct numbers of differentially expressed genes (DEGs) across distinct drugs (Table S1). Moreover, PDPCC primed with activating epidrugs presented a higher number of DEGs (2664.60 ± 1949.31 vs. 450.80 ± 693.09) and a bigger proportion of upregulated genes (60.58 ± 18.42% vs. 43.44 ± 28.36%) compared to PDPCCs primed with repressive epidrugs (Fig. 2a; Fig. S1a; $\chi2$ test p-value <0.01). DEG expression levels in individual patient-derived primary pancreatic cancer cell cultures for each epidrug showed an overall homogenous transcriptomic response to priming with only subtle differences (Fig. S1b). Further analysis revealed a positive correlation between the number of shared DEGs and pathways, in the epidrug-primed PDPCC (R = 0.40, p-value <0.006, Fig. S1c and S1d). The epidrug redundant effects were associated with a significant repression of the cell cycle pathways in epidrug-primed PDPCCs for 8 out of 10 epidrugs (Fig. 2b and Table S2). The importance of this novel observation is significant since, regardless of the final target, during a chemogenomic priming most of H3K9 and H3K27 enhancer-targeting drugs display an effect that primarily converges on cell cycle regulatory networks. We next evaluated the potential bias that could arise in gene expression levels caused by any difference in proliferation rates among PDPCCs. This control is important since cell density and contact can modify cell cycle. Thus, we compared the mean PDPCC doubling rate against gene expression levels observed upon priming (sum of absolute fold change of DEG) (Fig. S2). The Spearman correlation coefficient between the PDPCC doubling rate and their global epidrug-primed gene expression change was non-significant for practically all the epidrugs (9/10). We only found a surprising difference, for the OICR9429 epidrug, with a coefficient of −0.8 (p-value = 0.014), even though it shares the same target as the WDR50103 epidrug.

To evaluate whether priming impact the molecular phenotype of PDPCC's, we investigated the shift of the PDAC subtype (Basal-like vs. Classical) using the transcriptomic gradient approach[13,14] following priming (Fig. 2c). Interestingly, a statistically significant stronger dominance of a classical phenotype was observed in four out of ten epidrugs. We also found/a significant shift of PAMG and PAMGMR from the average measures for a classical phenotype in PDPCCs primed with only one compound. On the other hand, OICR9429 was the only epidrug with a shift to the basal-like subtype measured by PAMGMR (Fig. 2c). The rest of the drugs did not display a significant phenotype shift. Together, these results demonstrate that an effective chemogenomic response can be established for representatives of both pancreatic cancer phenotypic subtypes. More
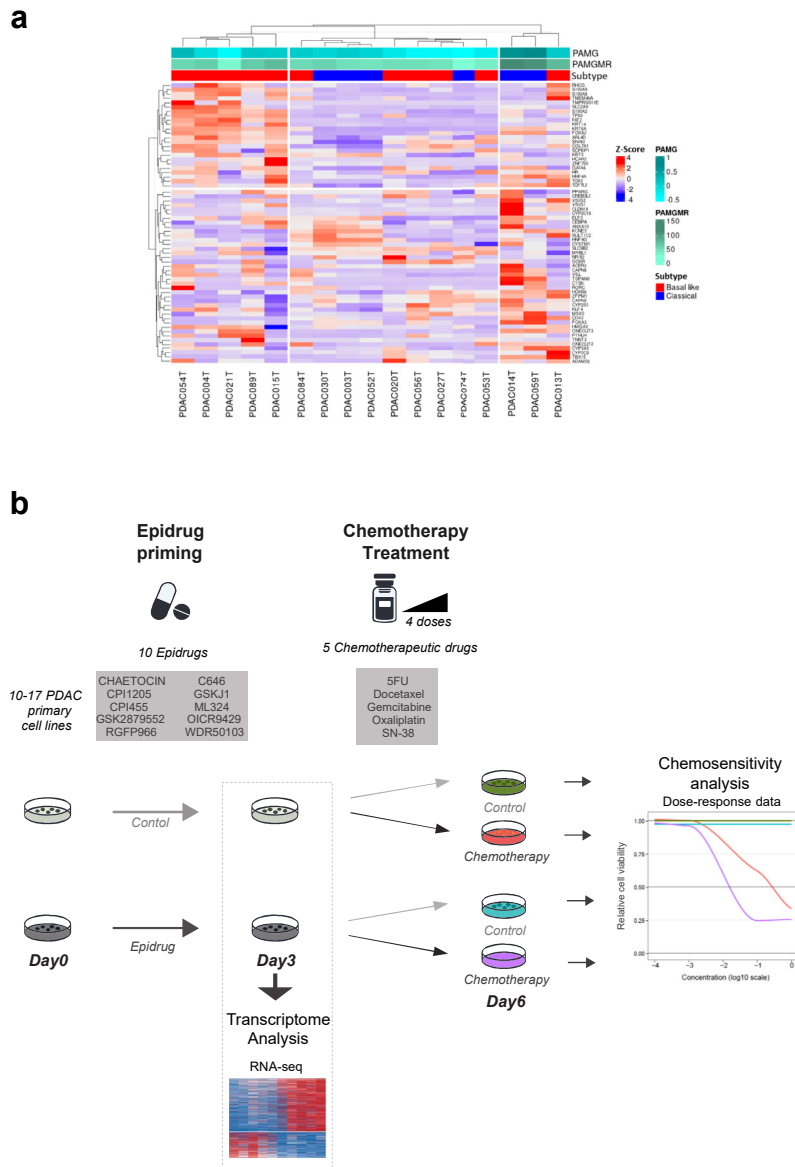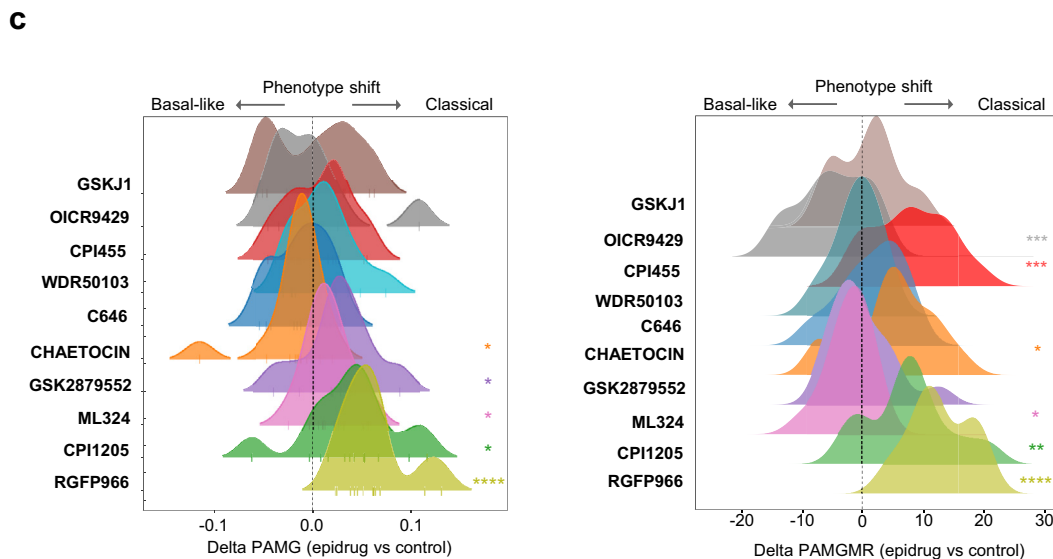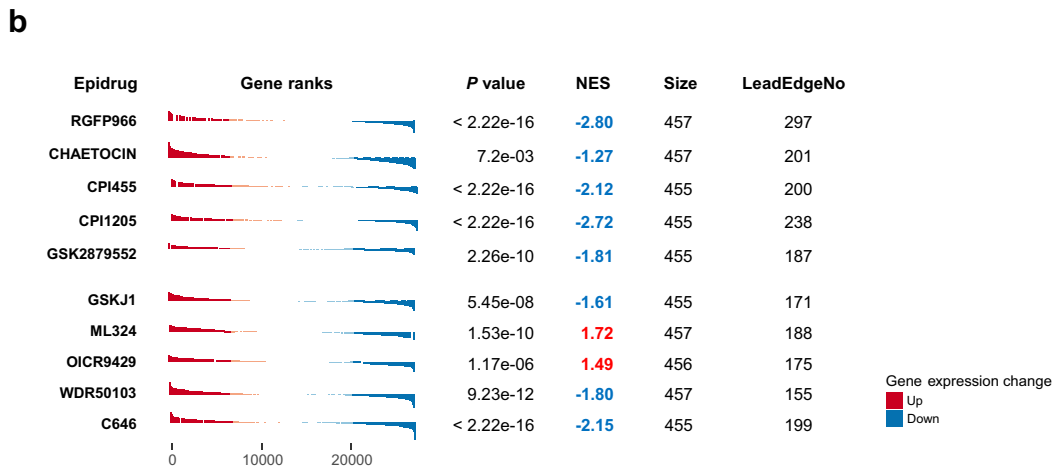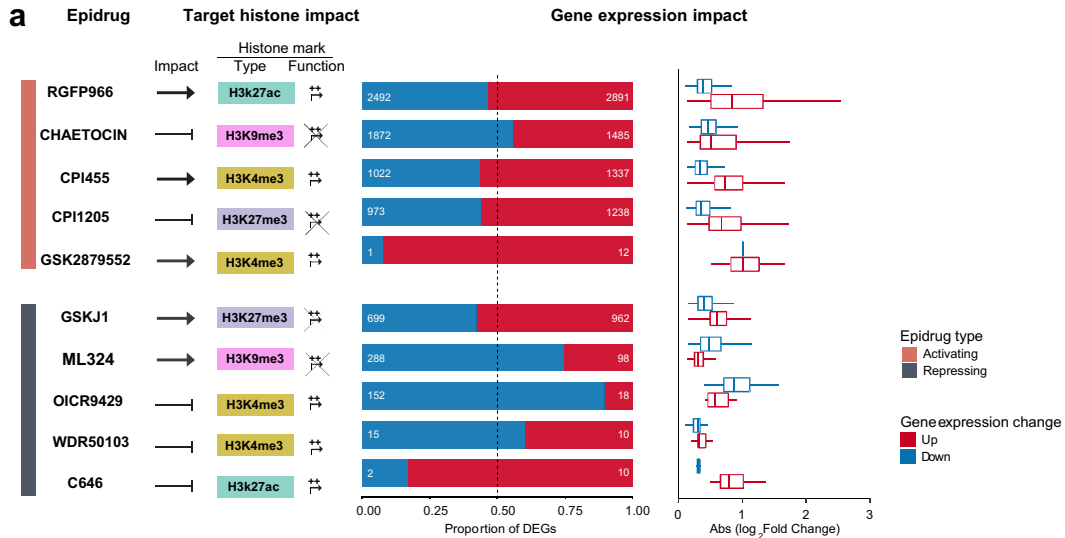
a

b

Fig. 1: Samples and experimental characterization. (a) Heatmap representing the classical and basal-like phenotype distribution of the PDAC-derived primary cell cultures (PDPCCs). (b) Experimental diagram showing that PDPCCs were pretreated with 10 different epidrugs for 72 h (epidrug priming). Following epidrug priming, cells were treated with 4 incremental doses of 5 distinct chemotherapeutic drugs for a further 72 h. Cells were counted at day 6 in order to assess the impact of pretreatment on chemosensitivity. Cell counts were normalized to the control group without epidrug and chemotherapeutic drug treatment. In an independent experiment, transcriptome analysis (RNAseq) was carried out on all cell lines that underwent epidrug pretreatment to determine signatures of response.

importantly, we find that, despite their primarily activating or repressing effects on gene expression, the shared effect of these drugs affects primarily cell cycle regulatory gene expression networks.

Evaluation of the predictive vs. empirical effects of enhancer targeting drugs

A common misconception is that epigenomic writers only modify histones. However, epigenomic enzymes also modify a myriad of proteins through histone-mimicry.[15–17] Thus, we defined whether the baseline epigenetic landscape of untreated PDAC cells predicts candidate genes that can be impacted by a given epidrug. Consequently, we identified the chromatin state significantly enriched around the transcription start site (TSS) of genes whose expression display significant likelihood of being modified by chemogenomic priming. We carried out gene set enrichment analysis

a

Epidrug		Target histone impact			Gene expression impact	

b

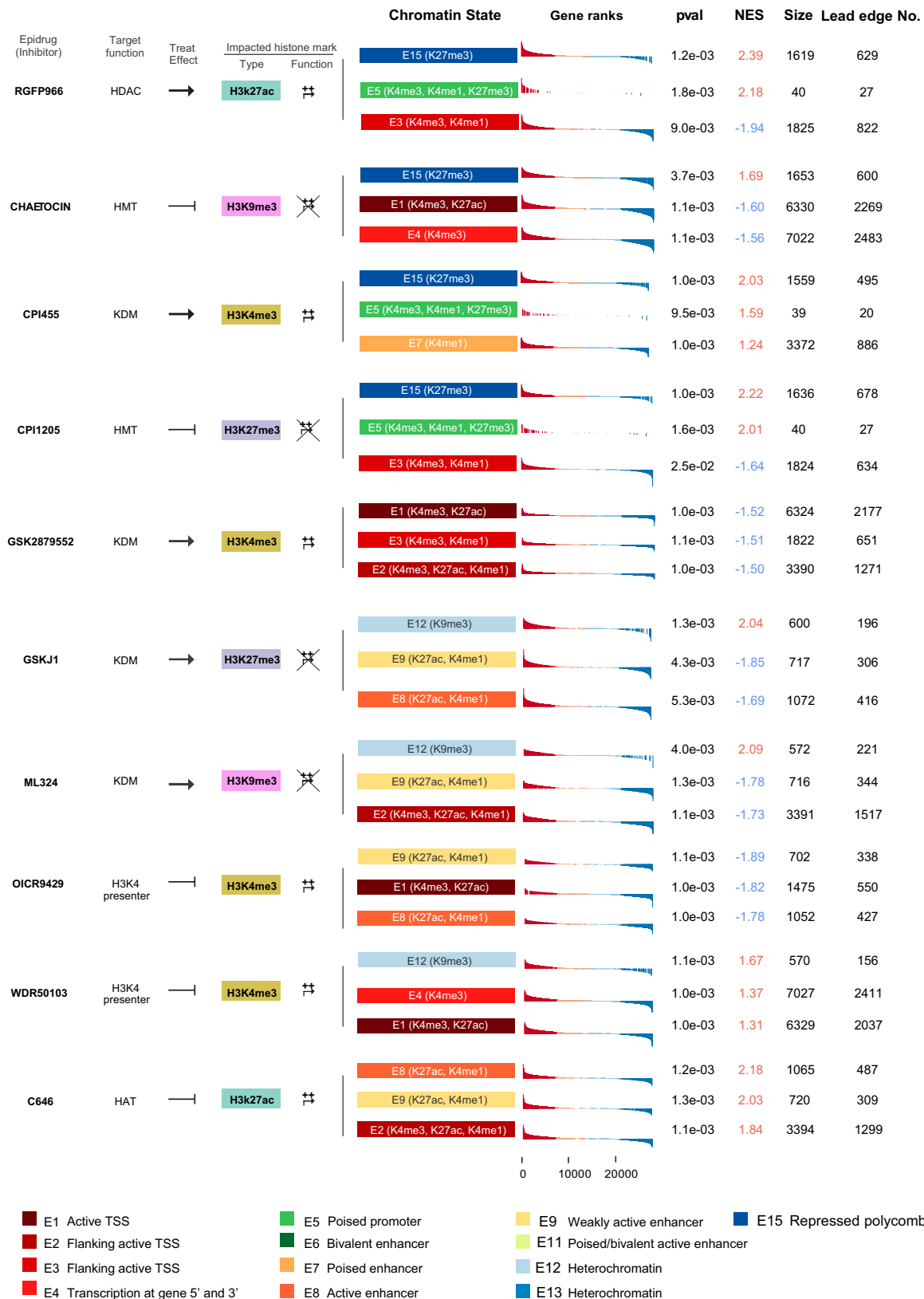| Epidrug	Gene ranks	P value	NES	Size	LeadEdgeNo
RGFP966		< 2.22e-16	-2.80	457	297
CHAETOCIN		7.2e-03	-1.27	457	201
CPI455		< 2.22e-16	-2.12	455	200
CPI1205		< 2.22e-16	-2.72	455	238
GSK2879552		2.26e-10	-1.81	455	187
GSKJ1		5.45e-08	-1.61	455	171
ML324		1.53e-10	1.72	457	188
OICR9429		1.17e-06	1.49	456	175
WDR50103		9.23e-12	-1.80	457	155
C646		< 2.22e-16	-2.15	455	199

c

(GSEA) using chromatin state baseline signatures identified in PDAC obtained by our group.[8] NES from the GSEA indicate an enrichment of the chromatin state in the TSS of highly expressed or under expressed genes containing the histone mark regulated by the epidrug-primed vs. control PDPCCs. CPI1205 and ML324 were the only epidrugs that showed a significant enrichment in the chromatin state specifically associated with their target histone mark with a NES of 2.22 and 2.09, respectively. The other epidrugs did not display a significant enrichment of chromatin states associated with target histone marks (Fig. 3). These results highlight that, during a chemogenomic priming event that spans at least one S phase but not numerous cell cycles, the effects of these epidrugs are significant but difficult to predict. This finding highlights the complexity of epigenetic enzyme targeting and the need of empirical experimentations to thoroughly investigate indirect effects created by histone mimicry and pathway cross-talks require empirical experimentations.

Chemogenomic priming changes chemosensitivity of human pancreatic cancer cells of different subtypes

To determine chemogenomic effects of the epidrugs priming on chemosensitivity of PDPCCs, we evaluated cell viability for each PDPCCs with chemotherapeutics alone, and chemogenomic priming followed by chemotherapeutics (referred to as EpiChemo). Note that EpiChemo differs from traditional combinatorial therapy in which two or more drugs are used simultaneously rather than sequentially. We defined chemosensitization by the chemogenomic priming of PDPCCs (induced by chemogenomic priming) using two scores, namely the SBliss synergy and the ECGain scores.[12,18] The SBliss score measures whether the EpiChemo treatment results in a synergic sensitization of PDPCCs compared to the independent effect of chemotherapy and chemogenomic priming alone. ECGain represents the global effect of the chemogenomic priming on chemotherapeutic efficacy. The ECGain score is important to compensate for the cases in which priming with certain chemogenomics

alone could result in a strong and dominating impact on PDPCC viability (4.3%). A SBliss score indicative of a synergic response, together with a high ECGain, reflects a stronger impact on PDPCC viability for a given Epi-Chemo compared to either of its components alone. Using the calculated SBliss and ECGain scores, we determined five different kinds of responses to Epi-Chemo treatment: a. Synergic, where the effect of the EpiChemo is higher than either treatment alone (SBliss ≥ 10% & ECGain ≥ 10%); b. Additive, where the effect of the EpiChemo is equivalent to the sum of the independent treatments (−10% ≤ SBliss <10% & ECGain ≥ 10%); c. Antagonistic, where the EpiChemo results in a smaller effect than the added effect of each treatment independently (mSBliss < −10% & ECGain ≥ 10%); d. Neutral, where the chemogenomic priming phase does not add any more benefit than chemotherapy alone (−10 < ECGain < 10) and e. Deleterious, where the EpiChemo leads to an increase in cell survival compared to either treatment alone (ECGain ≤ −10) (Fig. 4a). We consider synergic responses most likely reflect a beneficial chemosensitization effect of distinct chemogenomic agents. Regarding drug safety of the chemogenomic protocol, we did not detect deleterious responses, defined as those in which chemogenomic priming results in increased PDPCCs survival. Evaluation of the chemosensitization studies, however, demonstrated that 60% of the cells displayed decreased cell viability as result of either an additive (48.3%) or synergic effect (11.7%) of all samples (Fig. 4a; Table S3). Overall, 100% of PDPCCs were observed to be sensitizable by one type of chemogenomics. We also find that chemogenomics were the most beneficial in chemosensitazing PDPCCs to both SN-38 (20.0%) and gemcitabine (12.9%) whereas oxaliplatin (7.5%) was on the opposite spectrum of responses (Fig. 4b, left). The biggest chemosensitizations were caused by drugs targeting H3K27-mediated enhancer formation and enhancer-promoter coupling (p300-HDAC3-EZH2-KDM5A) with KDM4B-HDAC3 targeting H3K9 promoter functions (Fig. 4b, right). These results demonstrate the potential benefit of these chemogenomics to achieve chemosensitization.

Fig. 2: Epidrugs alone have a heterogenous impact on gene expression. (a) *Middle.* Number of genes having a significant (adjusted p-value ≤0.05) change of expression (upregulated in red, downregulated in blue) following treatment of PDPCCs with epidrug alone (10 epidrugs; 72 h). *Right.* Comparison of absolute fold change of expression (log2) of such significantly deregulated genes (outliers not shown; outliers defined as any data points 1.5 times below/above the interquartile range below/above the 25th/75th percentile, respectively). Color of bars indicates direction of change with respect to untreated cells. Results have been ordered within each global expected impact of epidrug treatment (activation or repression) based on epidrug's histone mark target and histone mark target function (*Left*). (b) Normalized Enrichment Score (NES) and associated p-values for the KEGG Cell Cycle Mitotic Pathway, after gene set enrichment analysis (GSEA) of PDPCCs treated with epidrug alone. GSEA was carried out on genes ranked on the Wald-statistic derived from the differential expression comparison between epidrug treated vs. control cells. Color of ranked genes indicates direction of change of expression (epidrug vs. control; upregulated in red, downregulated in blue). Pathway gene size and number of genes contributing the most to the enrichment of the pathway are shown. (c) Shift in Pancreatic Ductal Adenocarcinoma (PDAC) Molecular Gradient (PAMG) and PAMG Master Regulators (PAMGMR) after epidrug treatment of PDPCCs. The scores pre and post epidrug treatment were compared by Wilcoxon matched pairs signed rank test. Asterisks represent level of p-value significance: *, **, ***, ****: p-value <0.05, 0.01, 0.001, and <0.001.

Epidrug (Inhibitor)	Target function	Treat Effect	Impacted histone mark Type	Impacted histone mark Function	Chromatin State	Gene ranks	pval	NES	Size	Lead edge No.
RGFP966	HDAC	→	H3k27ac		E15 (K27me3)		1.2e-03	2.39	1619	629
					E5 (K4me3, K4me1, K27me3)		1.8e-03	2.18	40	27
					E3 (K4me3, K4me1)		9.0e-03	-1.94	1825	822
CHAETOCIN	HMT	⊣	H3K9me3		E15 (K27me3)		3.7e-03	1.69	1653	600
					E1 (K4me3, K27ac)		1.1e-03	-1.60	6330	2269
					E4 (K4me3)		1.1e-03	-1.56	7022	2483
CPI455	KDM	→	H3K4me3		E15 (K27me3)		1.0e-03	2.03	1559	495
					E5 (K4me3, K4me1, K27me3)		9.5e-03	1.59	39	20
					E7 (K4me1)		1.0e-03	1.24	3372	886
CPI1205	HMT	⊣	H3K27me3		E15 (K27me3)		1.0e-03	2.22	1636	678
					E5 (K4me3, K4me1, K27me3)		1.6e-03	2.01	40	27
					E3 (K4me3, K4me1)		2.5e-02	-1.64	1824	634
GSK2879552	KDM	→	H3K4me3		E1 (K4me3, K27ac)		1.0e-03	-1.52	6324	2177
					E3 (K4me3, K4me1)		1.1e-03	-1.51	1822	651
					E2 (K4me3, K27ac, K4me1)		1.0e-03	-1.50	3390	1271
GSKJ1	KDM	→	H3K27me3		E12 (K9me3)		1.3e-03	2.04	600	196
					E9 (K27ac, K4me1)		4.3e-03	-1.85	717	306
					E8 (K27ac, K4me1)		5.3e-03	-1.69	1072	416
ML324	KDM	→	H3K9me3		E12 (K9me3)		4.0e-03	2.09	572	221
					E9 (K27ac, K4me1)		1.3e-03	-1.78	716	344
					E2 (K4me3, K27ac, K4me1)		1.1e-03	-1.73	3391	1517
OICR9429	H3K4 presenter	⊣	H3K4me3		E9 (K27ac, K4me1)		1.1e-03	-1.89	702	338
					E1 (K4me3, K27ac)		1.0e-03	-1.82	1475	550
					E8 (K27ac, K4me1)		1.0e-03	-1.78	1052	427
WDR50103	H3K4 presenter	⊣	H3K4me3		E12 (K9me3)		1.1e-03	1.67	570	156
					E4 (K4me3)		1.0e-03	1.37	7027	2411
					E1 (K4me3, K27ac)		1.0e-03	1.31	6329	2037
C646	HAT	⊣	H3k27ac		E8 (K27ac, K4me1)		1.2e-03	2.18	1065	487
					E9 (K27ac, K4me1)		1.3e-03	2.03	720	309
					E2 (K4me3, K27ac, K4me1)		1.1e-03	1.84	3394	1299

Gene ranks axis: 0   10000   20000

Legend:
- E1 Active TSS
- E2 Flanking active TSS
- E3 Flanking active TSS
- E4 Transcription at gene 5' and 3'
- E5 Poised promoter
- E6 Bivalent enhancer
- E7 Poised enhancer
- E8 Active enhancer
- E9 Weakly active enhancer
- E11 Poised/bivalent active enhancer
- E12 Heterochromatin
- E13 Heterochromatin
- E15 Repressed polycomb

Next, we built a binary heatmap to compare chemo-sensitized PDPCCs shared by all EpiChemos (Fig. 4c). This calculation shows that 82% of EpiChemo combinations display synergic chemosensitization. We observe that the chemotherapeutic drug that becomes more beneficial, after chemogenomics, is SN-38. More importantly, most/all beneficial chemogenomic effects were achieved with drugs that target H3K27-mediated enhancer-promoter coupling (Fig. 4c and Fig. S3). This important result highlights the potential of exploring further chemogenomic protocols that can be used to repurpose already approved safe drugs for pancreatic cancer treatment with a precision medicine focus. Moreover, the fact that we rarely observed strong cyto-toxicity during the chemogenomic priming phase alone reveals the potential of generating lower systemic side effects.

Chemogenomic priming associates with distinct chemosensitization signatures

With the purpose of predicting which would be the most effective chemogenomic approach to apply to naïve PDPCCs in the future, we established gene signatures of synergic response (chemosensitization) for specific EpiChemos. As summarized in Fig. 5a, we carried out a differential analysis using the baseline transcriptome of untreated PDPCCs. We compared basal gene expression levels in chemosensitized vs. not chemosensitized PDPCCs. To identify chemosensitizable PDPCCs from new, untreated samples (naïve PDPCCs, n = 44), we built a predictor for every EpiChemo pair for which enough number of chemosensitized PDPCCs had been experimentally observed (≥2) and a minimal difference of gene expression between chemosensitized vs. non-chemosensitized PDPCCs had been found (≥50 DEGs; Fig. S4a). In brief, a nearest-centroid predictor was built as predictive signature with the expression mean of the 1000 most deregulated genes from the PDPCCs that displayed a synergy effect. Of interest, comparison of baseline expression levels between PDPCCs that were predicted to be amenable to che-mosensitization vs. those predicted not to be chemo-sensitizable were like those observed experimentally for the different signatures (Fig. 5c). Furthermore, vali-dating our predictor, we observed that naïve PDPCCs presenting the biggest delta in correlations for synergy

signatures were properly predicted in their response, as confirmed by responses in dose-response experiments (heatmap annotations, Fig. 5b). Next, we evaluated the usefulness of these signatures by performing 32 distinct dose-response assays of distinct priming-chemotherapy treatments on 17 different PDPCCs, exposed to Gem-citabine and SN-38, after pretreatment with four epi-drugs (Fig. S4b). Based on dose-response assays, we found that 18 primed-chemotherapeutic combinations yielded sensitizing scores (SBliss ≥ 10% & ECGain ≥ 10%), the remaining 14 were not (5 additive, 1 delete-rious, and 8 neutral). After that, we identified six sig-natures that displayed the highest association with the centroid of chemosensitization (R ≤ −0.80; p-value < 0.01; Fig. S4b). These six signatures were validated in six PDPCC, which showed an increase in their response to the chemotherapeutic drug (Fig. 6). Lastly, we analyzed the level of specificity of the six chemosensitization regimen for the tumoral epithelial cells in two primary cancer-associated fibroblasts (CAFs), R1 and R2. We did not observe significant differences between the control (chemotherapeutic alone) and the EpiChemo combina-tions (Fig. S5), suggesting the selectivity of the epidrug priming approach.

Discussion

We have previously demonstrated that epigenomic pathways, those mediated by H3K9 and H3K27 en-hancers, drive differentiation of PDAC cells into sub-types. The current study makes additional advances to the field by conceptualizing and standardizing a che-mogenomic priming approach for briefly reprograming the transcriptional landscape of pancreatic cancer cells in manners that render them more sensitive to currently used, clinically approved drugs, with otherwise marginal effects on this disease. Our design involved the use of well-tested inhibitors for these enhancer regulatory pathways on a comprehensive set of patient-derived, primary, pancreatic cancer cell cultures of both clas-sical and basal PDAC subtypes. The bioinformatic approach reveals distinct and shared features of tran-scriptional landscapes that define each chemogenomic priming event in both subtypes. Moreover, we estab-lished gene signatures that enable the prediction of the chemosensitization effect. Thus, it becomes important

Fig. 3: Epidrug treatment results in enrichment of chromatin states defined by histone marks not directly targeted by the epidrug. *Right.* Chromatin states were defined in our previous work.[8] Top three chromatin states (most associated histone marks in brackets) found to be the most significantly enriched (GSEA) in genes ranked on Wald-statistic from differential analysis of epidrug treated PDPCCs (epidrug vs. control). Normalized Enrichment Score (NES), size of genes associated to the mark and number of genes contributing the most to the enrichment (leading edge) are displayed. Enrichment of chromatin states was assessed for each epidrug at a proximal distance from the transcription start site (TSS). Proximal distance: 2 kb upstream TSS; 500 bp downstream TSS. Color of ranked genes and NES are indicative of direction of change of expression between epidrug-treated vs. ctrl PDPCCs. *Left.* For each epidrug, the functional class of its directly inhibited target is shown, followed by the impacted histone mark and its function (repression: crossed arrow; activation: uncrossed arrow). Global impact on gene expression for each epidrug is indicated based on histone mark target and function.
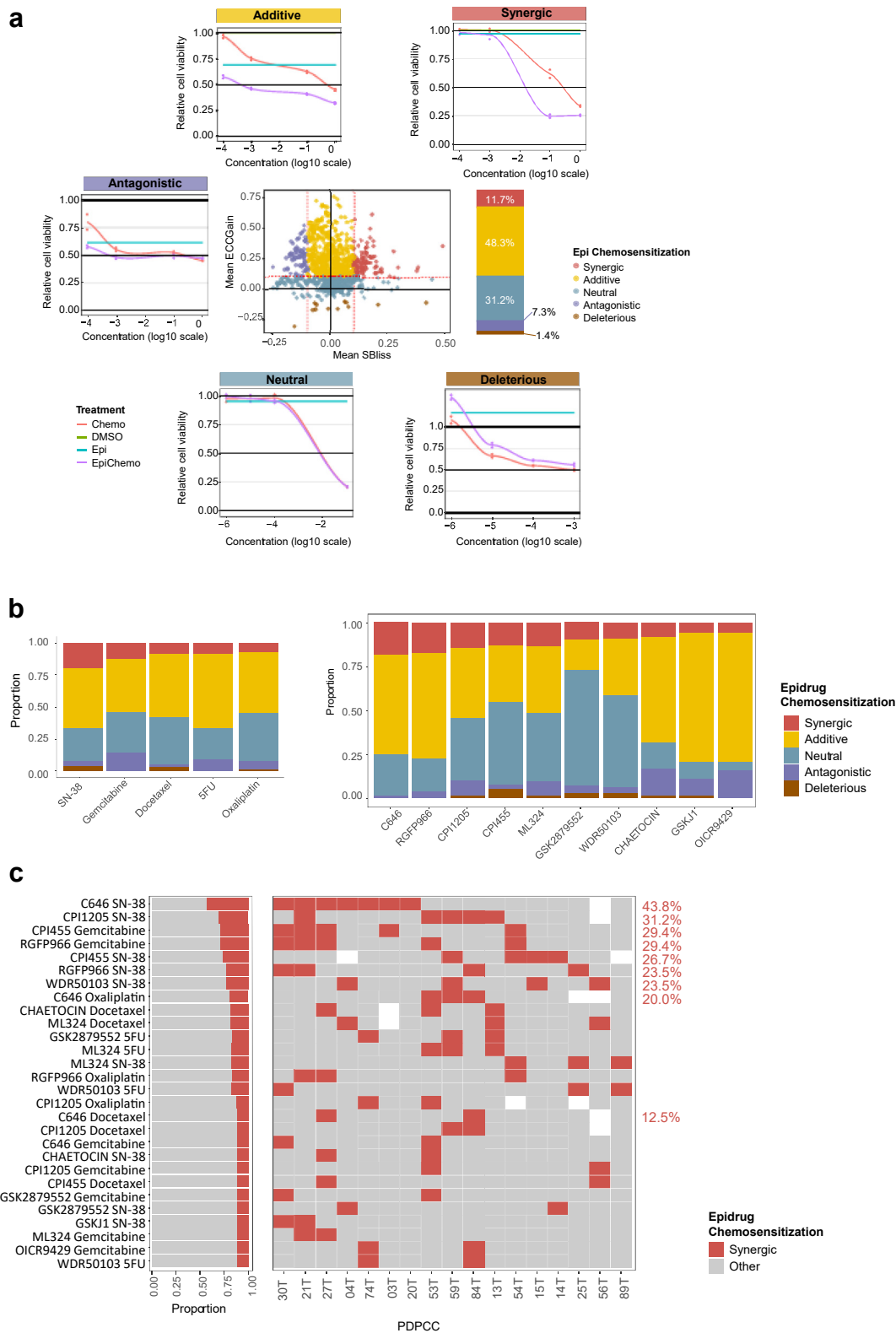
Fig. 4: Evaluation of the effect of epidrug priming in PDPCCs treated with incremental doses of chemotherapy. (a) Establishment of type of response due to epidrug priming of PDPCCs using synergy Bliss score (SBliss) and gain of detrimental impact on cell proliferation (ECCGain).
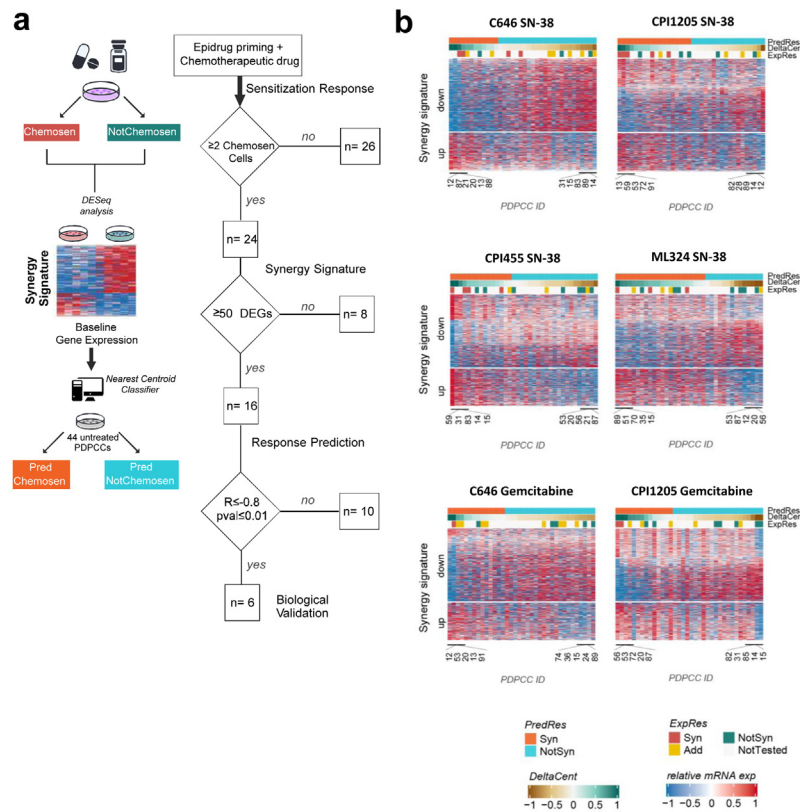
Fig. 5: Synergy (chemosensitization) signatures enable the devising of a nearest centroid classifier used to predict chemosensitizing response in untreated PDPCCs. (a) Flow diagram illustrating the establishment of synergic response gene signatures for selected EpiChemo treatments. As a first step, EpiChemo treatments were chosen based on the number of PDPCCs that were or not experimentally chemosensitized (at least 2 chemosensitized PDPCCs cells). Synergic response signatures (Synergy signatures) were identified from the differential analysis of baseline gene expression between chemosensitized vs. not-chemosensitized PDPCCs (ChemoSen and NotChemosen, respectively). EpiChemo synergy signatures for which there was a significant difference of expression (≥50 DEGs) between ChemoSen vs. NotChemosen cells were further used to build a predictor (nearest centroid classifier) using the top 1000 most deregulated genes. New, untreated PDPCCs (n = 44) were predicted to be chemosensitized or not based on the closeness of their expression profiles to the established centroids. A final selection was done to determine the EpiChemos that would be functionally validated (significant negative correlation between expression profile distances to ChemoSen vs. NotChemoSen centroids; R ≤ –0.8, p-value ≤0.01; n = 6). (b) Synergy signature expression heatmaps for six EpiChemos (to be functionally validated) in the 44 treatment-naive PDPCCs. The IDs of the top ten PDPCCs presenting the strongest delta of correlations to the Syn and NotSynCell centroids are displayed. Synergy signature genes are ordered according to observed delta of expression when defining signatures (ChemoSen vs. NotChemosen PDPCCs). The prediction of the centroid classifier (predicted ChemoSen vs. predicted NotChemosen) is shown above each PDPCC. In case the PDPCC was previously treated with a given EpiChemo, the experimentally observed response is indicated (Add: additive; Syn: Synergic). DEGs: differentially expressed genes.

Center. Scatter plot comparing mean SBliss and ECCGain for every (pre)treatment set of PDPCC (epidrug priming + chemotherapeutic drug; n = 830). Color of dots denotes assigned response type. *Periphery.* Representative dose response curves for each of the identified response types. Impact on cell proliferation is shown and compared between control (DMSO), epidrug alone (Epi), chemotherapeutic drug alone (Chemo), and epidrug-primed + chemotherapy (EpiChemo) treated PDPCCs. Chemo and EpiChemo samples were analyzed at four different doses of a chemotherapeutic drug. All curves are normalized to control. Dose response curves for the different response types do not represent the same PDPCC, epidrug nor chemotherapeutic drug. (b) Stacked barplots showing percentage of samples presenting the different kinds of responses for every individual chemotherapeutic drug (*Left*) or epidrug (*Right*). (c) *Center.* Binary heatmap indicating if (pre)treatment of a PDPCC with a given EpiChemo resulted in a chemosentitization (synergic response: red tiles; gray tiles indicate non synergic response). *Top.* For every PDPCC, percent of EpiChemo regimes that resulted in a synergic chemosensitization. *Right.* For every EpiChemo, percentage of different response types. EpiChemos are ordered from highest to lowest proportion of chemosensitized PDPCCs. Are only displayed EpiChemos resulting in chemosensitization of at least 2 PDPCCs.
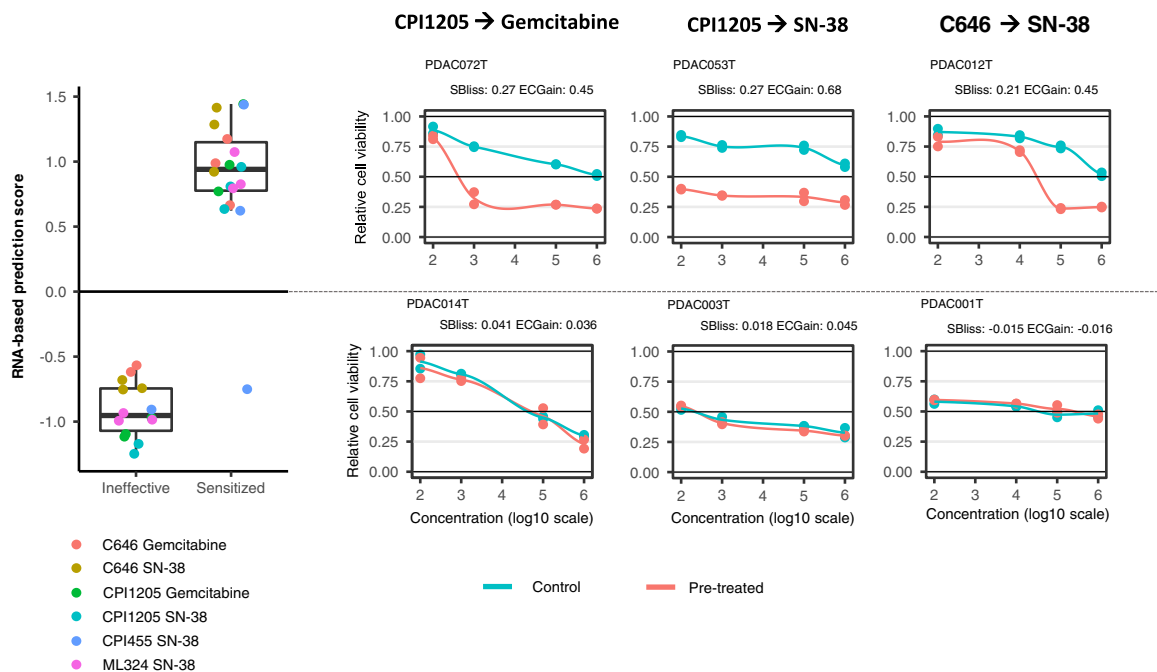
Fig. 6: Experimental validation of synergy signatures. Distribution of the RNA-based chemosensitization signature scores for 32 assays (17 different PDPCCs) classified as effectively chemosensitized (SBliss ≥ 10% & ECGain ≥ 10%) or ineffective chemosensitization. Assay dots are identified by the Epidrug-chemotherapy pair for which the specific RNA signature was used, and the epidrug-priming was performed. Dose-response of the corresponding assays are shown.

to discuss the implications of these study to PDAC pathobiology and therapeutics.

One important observation of support one guiding hypothesis of our study is that chemogenomic priming with these enhancer-targeting drugs is difficult to predict based on chromatin state alone and must be evaluated empirically. Together, these results demonstrate that an effective chemogenomic response can be established for representatives of both pancreatic cancer phenotypic subtypes. More importantly, we find that, despite their primarily activating or repressing effect on gene expression, the shared chemogenomic effect of these drugs affects primarily cell cycle regulatory gene expression networks. In fact, because the epigenome maintains content epigenomes landscape with their corresponding transcriptional profile, we predicted responses based on a couple of logical criteria, namely 1. Similar cancer cell subtype would display a similar pattern of response to a distinct drug; 2. Some drugs would primarily exert a positive or negative effect on H3K9 and H3K27 enhancers, enriching the resulting landscapes primarily with downregulated or upregulated genes; and 3. Some communality should be found among all drugs during the chemogenomic priming period.

We observed a heterogeneity of response among the different epidrugs, which could be explained by distinct gene target selectivity for each epidrug, as previously described by Sato et al. in epidrug treated colon, breast and leukemia cancer cell lines.[19] Despite observing such heterogeneity of transcriptomic impact, gene set enrichment analysis led us to identify the cell cycle as the pathway that was significantly altered by all epidrugs (repressed by 8/10 epidrugs). Supporting our results, similar effects on the cell cycle have been reported for different epidrug/histone-modifying-enzyme-invalidation treatments in several PDAC in vitro models.[20–22] Drug targeting epigenetic regulators such as histone modifying enzymes has long been described as challenging due to the existence of an intricate histone interaction network involving cross-talk mechanisms between histone acetylation and methylation as well as interactions with many non-histone proteins.[23,24] As an example, Huang et al. reported that HDAC inhibitors not only increase acetylation of H3 histones but also favor their methylation in prostate cancer cell lines, via repression of H3K4 demethylases.[25] In other studies, inhibition of HATs with ICG-001 and C646 led to a significant change of global H3K27ac and H3k4me3 levels in the pancreatic PANC1 cell line.[26] In agreement with these reports, we confirmed in the present study that the genes exhibiting a change in expression following epidrug priming were enriched in histone marks and associated chromatin states different to the initial targeted enzyme. Although at first sight epidrug priming of our PDPCCs resulted in the chemosensitizer

effect (synergic response) of only 11% of samples (n = 830), treatment of PDPCCs with three different EpiChemo combinations (C646/SN-38, CPI1205/SN-38, and CPI455/SN-38) led to the chemosensitization of more than 80% of primary cell cultures, highlighting the chemosensitizing potential of epidrug priming in PDAC. So far, only two previous studies in PDAC cell lines have demonstrated an increase in cell cytotoxicity following the combined treatment of gemcitabine with either C646 or DZNeP (EZH2 inhibitor).[27,28] Such results are very promising; however, care must be taken to reduce the possible systemic toxicities that have been frequently reported in epigenetic drug + chemotherapy combination trials for many other cancer types.[29] In our model, pretreating PDPCCs first with the epidrug alone (epidrug priming) and then treating with the chemotherapeutic drug may offer a possibility of reducing unwanted toxicities whilst still allowing for a synergic chemosensitization of PDAC patients. However, despite the promising results displayed here, it is important to highlight that our results are limited to 17 PDPCCs only. Thus, further validation on in vivo and in vitro models is necessary to confirm our observations. Moreover, the epidrugs used in this study are not clinically available and, in some cases, have shown off-target effects (Table S4). Hence is necessary to expand the scope of our analysis to targets with clinically available compounds.

In summary, the current study demonstrated that modulating the epigenomic landscape through epidrugs improves the PDAC response to the current treatments in PDPCCs. Moreover, we proposed a transcriptomic signature to select the responder tumors.

References

1 Sung H, Ferlay J, Siegel RL, et al. Global cancer statistics 2020: GLOBOCAN estimates of incidence and mortality worldwide for 36 cancers in 185 countries. *CA Cancer J Clin*. 2021;71:209–249. https://doi.org/10.3322/caac.21660.

2 Carioli G, Malvezzi M, Bertuccio P, et al. European cancer mortality predictions for the year 2021 with focus on pancreatic and female lung cancer. *Ann Oncol*. 2021;32:478–487. https://doi.org/10.1016/j.annonc.2021.01.006.

3 Mizrahi JD, Surana R, Valle JW, Shroff RT. Pancreatic cancer. *Lancet*. 2020;395:2008–2020. https://doi.org/10.1016/S0140-6736(20)30974-0.

4 Swayden M, Iovanna J, Soubeyran P. Pancreatic cancer chemo-resistance is driven by tumor phenotype rather than tumor genotype. *Heliyon*. 2018;4:1055. https://doi.org/10.1016/j.heliyon.2018.e01055.

5 Nicolle R, Blum Y, Marisa L, et al. Pancreatic adenocarcinoma therapeutic targets revealed by tumor-stroma cross-talk analyses in patient-derived xenografts. *Cell Rep*. 2017;28:2458–2470. https://doi.org/10.1016/j.celrep.2017.11.003.

6 Witkiewicz AK, Balaji U, Eslinger C, et al. Integrated patient-derived models delineate individualized therapeutic vulnerabilities of pancreatic cancer. *Cell Rep*. 2016;16:2017–2031. https://doi.org/10.1016/j.celrep.2016.07.023.

7 Lomberk G, Dusetti N, Iovanna J, Urrutia R. Emerging epigenomic landscapes of pancreatic cancer in the era of precision medicine. *Nat Commun*. 2019;10:3875. https://doi.org/10.1038/s41467-019-11812-7.

8 Lomberk G, Blum Y, Nicolle R, et al. Distinct epigenetic landscapes underlie the pathobiology of pancreatic cancer subtypes. *Nat Commun*. 2018;9:1978. https://doi.org/10.1038/s41467-018-04383-6.

9 Cheng Y, He C, Wang M, et al. Targeting epigenetic regulators for cancer therapy: mechanisms and advances in clinical trials. *Signal Transduct Targeted Ther*. 2019;4:1–39. https://doi.org/10.1038/s41392-019-0095-0.

10 McCleary-Wheeler AL, Lomberk GA, Weiss FU, et al. Insights into the epigenetic mechanisms controlling pancreatic carcinogenesis. *Cancer Lett*. 2013;328:212–221. https://doi.org/10.1016/J.CANLET.2012.10.005.

11 Leca J, Martinez S, Lac S, et al. Cancer-associated fibroblast-derived annexin A6+ extracellular vesicles support pancreatic cancer aggressiveness. *J Clin Invest*. 2016;126:4140–4156. https://doi.org/10.1172/JCI87734.

12 Bliss CI. The toxicity of poisons applied jointly. *Ann Appl Biol*. 1939;26:585–615. https://doi.org/10.1111/J.1744-7348.1939.TB06990.X.

13 Fraunhoffer NA, Abuelafia AM, Bigonnet M, et al. Multi-omics data integration and modeling unravels new mechanisms for pancreatic cancer and improves prognostic prediction. *NPJ Precis Oncol*. 2022;6:57. https://doi.org/10.1038/s41698-022-00299-z.

14 Nicolle R, Blum Y, Duconseil P, et al. Establishment of a pancreatic adenocarcinoma molecular gradient (PAMG) that predicts the clinical outcome of pancreatic cancer. *EBioMedicine*. 2020;57:102858. https://doi.org/10.1016/j.ebiom.2020.102858.

15 Biggar KK, Li SSC. Non-histone protein methylation as a regulator of cellular signalling and function. *Nat Rev Mol Cell Biol*. 2014;16:5–17. https://doi.org/10.1038/nrm3915.

16 Singh BN, Zhang G, Hwa YL, Li J, Dowdy SC, Jiang SW. Nonhistone protein acetylation as cancer therapy targets. *Expert Rev Anticancer Ther*. 2014;10:935–954. https://doi.org/10.1586/ERA.10.62.

17 Bondy-Chorney E, Denoncourt A, Sai Y, Downey M. Nonhistone targets of KAT2A and KAT2B implicated in cancer biology. *Biochem Cell Biol*. 2019;97(1):30–45. https://doi.org/10.1139/bcb-2017-0297.

18 Malyutina A, Majumder MM, Wang W, Pessia A, Heckman CA, Tang J. Drug combination sensitivity scoring facilitates the discovery of synergistic and efficacious drug combinations in cancer. *PLoS Comput Biol*. 2019;15:e1006752. https://doi.org/10.1371/JOURNAL.PCBI.1006752.

19 Sato T, Cesaroni M, Chung W, et al. Transcriptional selectivity of epigenetic therapy in cancer. *Cancer Res*. 2017;77:470–481. https://doi.org/10.1158/0008-5472.CAN-16-0834.

20 Gaddis M, Gerrard D, Frietze S, Farnham PJ. Altering cancer transcriptomes using epigenomic inhibitors. *Epigenet Chromatin*. 2015;8:1–12. https://doi.org/10.1186/1756-8935-8-9.

21 Mathison A, Salmonson A, Missfeldt M, et al. Combined AURKA and H3K9 methyltransferase targeting inhibits cell growth by inducing mitotic catastrophe. *Mol Cancer Res*. 2017;15:984–997. https://doi.org/10.1158/1541-7786.MCR-17-0063.

22 Tiffon C. Histone deacetylase inhibition restores expression of hypoxia-inducible protein NDRG1 in pancreatic cancer. *Pancreas*. 2018;47:200–207. https://doi.org/10.1097/MPA.0000000000000982.

23 Weigt D, Hopf C, Médard G. Studying epigenetic complexes and their inhibitors with the proteomics toolbox. *Clin Epigenet.* 2016;8(1):1–16. https://doi.org/10.1186/S13148-016-0244-Z.

24 Latham JA, Dent SYR. Cross-regulation of histone modifications. *Nat Struct Mol Biol.* 2007;14(11):1017–1024. https://doi.org/10.1038/nsmb1307.

25 Huang PH, Chen CH, Chou CC, et al. Histone deacetylase inhibitors stimulate histone H3 lysine 4 methylation in part via transcriptional repression of histone H3 lysine 4 demethylases. *Mol Pharmacol.* 2011;79:197–206. https://doi.org/10.1124/MOL.110.067702.

26 Gerrard DL, Boyd JR, Stein GS, Jin VX, Frietze S. Disruption of broad epigenetic domains in PDAC cells by HAT inhibitors. *Epigenomes.* 2019;3:11. https://doi.org/10.3390/EPIGENOMES3020011.

27 Ono H, Basson MD, Ito H, Ono H, Basson MD, Ito H. P300 inhibition enhances gemcitabine-induced apoptosis of pancreatic cancer. *Oncotarget.* 2016;7:51301–51310. https://doi.org/10.18632/ONCOTARGET.10117.

28 Avan A, Crea F, Paolicchi E, et al. Molecular mechanisms involved in the synergistic interaction of the EZH2 inhibitor 3-deazaneplanocin A with gemcitabine in pancreatic cancer cells. *Mol Cancer Ther.* 2012;11:1735–1746. https://doi.org/10.1158/1535-7163.MCT-12-0037/84448/AM/MOLECULAR-MECHANISMS-INVOLVED-IN-THE-SYNERGISTIC.

29 Morel D, Jeffery D, Aspeslagh S, Almouzni G, Postel-Vinay S. Combining epigenetic drugs with other therapies for solid tumours — past lessons and future promise. *Nat Rev Clin Oncol.* 2019;17(2):91–107. https://doi.org/10.1038/s41571-019-0267-4.